

## ELECTRODE PROCESSES AND SEM/EDX ANALYSIS OF SELENIUM FILMS ELECTRODEPOSITED FROM IONIC LIQUIDS BASED ON CHOLINE CHLORIDE

A. COJOCARU, I. SIN\*, C. AGAPESCU, A. COTARTA, T. VISAN

*Department of Inorganic Chemistry, Physical Chemistry and Electrochemistry,  
University POLITEHNICA of Bucharest, Romania*

The electrode processes of  $\text{Se}^{4+}$  at 60°C in three ionic liquids which consisted in eutectic mixtures of choline chloride with urea (ChCl-urea), ethylene glycol (ChCl-EG) or oxalic acid (ChCl-OxA) have been studied by cyclic voltammetry.  $\text{SeO}_2$  was the dissolved precursor in electrolyte and platinum and glassy carbon were the working electrodes. Successive processes of underpotential deposition, bulk deposition and conversion of  $\text{Se}^0$  into a soluble species ( $\text{Se}^{2-}$ ) were evidenced by gradual scanning of potential to more negative values. Using the same ionic liquids, selenium films have been prepared on copper substrate by electrolysis with controlled cathodic potential at 60 °C. Scanning electron microscopy and energy dispersive X-rays spectroscopy elemental analysis were carried out in order to evidence the dependences of morphology and chemical composition of Se films on nature of electrolyte and applied polarization potential.

(Received January 26, 2016; Accepted March 30, 2016)

*Keywords:* Selenium, Thin films, Electrodeposition, Ionic liquids, Choline chloride, SEM microscopy, EDX analysis

### 1. Introduction

Selenium is an indirect semiconductor with a narrow band gap of ~1.7eV (that may increase up to 3.0 eV) and a relatively high-ionization energy [1,2]. Selenium films have internal strong bonds tending to form polyatomic chains. Particularly, the interest in Se films is associated to promising physical properties [3-6] such as photoconductivity, superconductivity, piezoelectric effect, non-linear optical response, anisotropic thermoconductivity, thermoelectrical properties. They have also catalytic activity towards hydration and oxidation reactions of organic compounds. Fabricating Se into various types of nanostructures (nanoparticles, nanotubes, nanorods) may introduce new types of applications in solar cells (photoelectrodes), semiconductor rectifiers, photographic exposure meters, and xerography [3-9]. Elemental selenium can adopt an amorphous phase (coloured red, brown or black) and multiple allotropic crystalline modifications: three monoclinic  $\text{Se}_8$  phases, a rhombohedral  $\text{Se}_6$ , an orthorhombic Se, two cubic Se phases, and a hexagonal phase (called also 'trigonal' or 'metallic') [10-14]. Due to its property of reversible transformations between the amorphous and crystalline phases, Se is used in optical memory applications. At room temperature the most stable phase is the amorphous red selenium which is poorly conductive. The grey crystalline hexagonal phase is a stable semiconductor at temperature above 100°C. All the other phases are electrical insulators.

Electrochemical deposition has been widely employed in the manufacturing of elemental selenium as well as binary, ternary or even more complex compounds of selenium [15,16]. This technique is advantageous mainly due to simplicity, cost effectiveness and easy maintenance. The film thickness, chemical composition, morphology and microstructure of the deposited materials could be controlled by adjusting the parameters of the electrodeposition process.

Until now, the grey selenium which is the densest phase was prepared electrochemically from aqueous media using very acidic baths (sulfuric, hydrochloric, perchloric or nitric acids) with

---

\*Corresponding author: ion\_sin@yahoo.com

high precursor concentration and at temperature typically around 100°C [10]. The mechanism of  $\text{Se}^{4+}$  reduction in these media has been debated extensively in the last four decades [12-29]. Kowalik [30] has provided recently a thorough literature-based review on the complex voltammetric behaviour of  $\text{H}_2\text{SeO}_3$  species. The cyclic voltammetry results were interpreted in terms of a two-step reduction scheme: first process is a  $\text{Se}^0$  deposition,



followed by a subsequent reduction at more negative potentials,



The second process means an electrochemical dissolution of the solid selenium deposit and gaseous  $\text{H}_2\text{Se}$  formation in aqueous solutions. According to Wei et al. [17] and Lai et al. [28] a cathodic process generating directly  $\text{Se}^{2-}$  soluble species,



is very likely to undergo in competition to elemental  $\text{Se}^0$  deposition (process 1). Moreover, additional electrochemical quartz crystal microbalance measurements [30] have shown that Se starts to deposit again after the processes (2) or (3), with a very high precipitation rate, if the potential is maintained to excessive negative potentials. This is a proof that the presence of  $\text{Se}^{2-}$  soluble species enables the synproportionation (comproportionation) reaction:



Also, the mechanism of Se electrodeposition and structure of deposit strongly depend on the material of electrodes. Se element may react with substrate leading to the formation of insoluble selenide [27,30]. Therefore, to investigate the Se electrochemistry, mostly gold [17,18,21,24,26,27], platinum [21,22,25], tin dioxide [28] and glassy carbon [17,29] electrodes were used due to their wide electrochemical window and very weak reactivity. On voltammograms, first peaks or plateaus that occurred at the scan beginning are surface limited processes and represent the underpotential deposition of selenium, Se-UPD [23,30]. Further, bulk deposition takes place but this growth of Se film is stopping at a limiting thickness. Se deposits are grown again in the 'transpassive' potential domain [20].

Endres and his group [31-36] demonstrated that selenium can be easily electrodeposited from ionic liquids that consist in methylpyrrolidinium or methylimidazolium trifluoromethylsulfonate derivatives. These traditional ionic liquids have a wide electrochemical window and extremely low vapour pressures, which allow direct deposition of grey Se at temperature above 100°C. Endres et al. [31-33] prepared Se films at 70–100°C using 1-butyl-1-methylpyrrolidinium bis(trifluor-methylsulfonyl) amide (symbolized [BMP]Tf2N) in which  $\text{SeCl}_4$  precursor was dissolved. The influence of electrolysis parameters, such as time and temperature of bath, on the crystallinity of hexagonal and rhombohedral Se phases was studied. It was showed that the addition of 5 vol.% water in [BMP]Tf2N has a good influence to the crystallinity of film [34,35]. The same research group has studied comparatively the electrochemical behavior of  $\text{H}_2\text{SeO}_3$  in 1-ethyl-3-methyl-imidazolium trifluoromethylsulfonate at room and elevated temperatures (70, 90 and 110°C) using gold and copper substrates [36]. Also, researches performed by Chou et al. [37] and Steichen and Dale [38] have focused on the influence of precursor chemical nature ( $\text{SeCl}_4$  or  $\text{SeO}_2$ ) on the morphology and crystallinity of Se deposits prepared from 1-ethyl-3-methylimidazolium tetrafluoroborate/chloride.

New ionic liquids based on choline chloride (IUPAC name: 2-hidroxy-ethyl-trimethyl ammonium chloride) were recently found to have interesting perspectives in electrodeposition of selenium. In general, an eutectic-containing ionic liquid is formed due to the hydrogen bonds between choline chloride (ChCl) and amides, alcohols or carboxylic acids [39]. These binary mixtures are also called 'deep eutectic solvents' (DESs), being potentially recyclable,

biodegradable and with no harm on human health. For instance, the eutectic mixture of ChCl with urea can represent a green alternative in electrodeposition of CuInSe<sub>2</sub> and Cu(In,Ga)Se<sub>2</sub> films for photovoltaic applications [40].

Up to this moment one can find that only few studies on Se electrodeposition from DESs have been conducted. Very recently, Bougouma et al. [41] has reported the electrochemical behaviour of Se<sup>4+</sup> in choline chloride - urea eutectic with a single concentration of precursor (10 mM SeO<sub>2</sub>) using gold electrode in a temperature range from 70 to 110°C. Cyclic voltammetry and chronoamperometry techniques were employed within this temperature range. Similarly to aqueous solutions, three main cathodic peaks recorded were interpreted as Se-UPD, bulk deposition of Se (process 1) and subsequent reduction of the solid deposit leading to Se<sup>2-</sup> soluble species (process 2). By measuring the charges associated with the voltammetric peaks, the conclusion was that a six-electron direct reduction (process 3) is excluded. Some preliminary studies performed in our laboratory regarding Se electrodeposition at constant temperature (60°C) in eutectics consisted in mixtures of choline chloride with urea or ethylene glycol were reported previously [42]. The applied techniques were cyclic voltammetry (CV) and electrochemical impedance spectroscopy (EIS). Also, deposition of selenium as a component in BiTeSe [43,44] or BiSe [45] semiconductor films was discussed recently in other papers published by our group.

In this work, we present CV curves obtained at 60°C with platinum and glassy carbon (GC) electrodes, regarding electrochemical behavior of Se<sup>4+</sup> in three ionic liquids, namely mixtures of choline chloride with urea (ChCl-urea), ethylene glycol (ChCl-EG) or oxalic acid (ChCl-OxA). After establishing the appropriate potential range for Se electrodeposition, selenium films were electrodeposited on copper substrate and analysed by SEM microscopy and energy dispersion X-rays spectroscopy (EDX). To the best of the knowledge of the authors, the electrochemical properties of Se<sup>4+</sup> species, preparation of Se films and their microscopy analysis have not been systematically studied in the above three ionic liquids.

## 2. Experimental works

Background electrolytes were mixtures of choline chloride with urea (1:2 mole ratio), ethylene glycol (1:2 mole ratio) or dihydrate oxalic acid (1:1 mole ratio), respectively. All reagents for preparation of these ionic liquids were of analytical grade (Aldrich) and used in the experiments as purchased. Each binary mixture was heated at above 90°C for 30 min until homogeneous colourless liquid is formed and this remained stable at room temperature. SeO<sub>2</sub> (Alfa Aesar) was the precursor for dissolved free selenide ions. The Se<sup>4+</sup> molarities were calculated using density determined in our lab.

Cyclic voltammograms (2-100 mVs<sup>-1</sup> scan rates) were recorded using a potentiostat (SP150 Bio-Logic Sci. Instr. or Zahner elektrik IM 6e). The working electrode was a platinum plate (0.5 cm<sup>2</sup>) or disk (0.07 cm<sup>2</sup>); a glassy carbon disk (GC, 0.07 cm<sup>2</sup>) was also used as inert working electrode. A Pt plate with large surface area and an Ag wire were auxiliary electrode and reference electrode, respectively.

In order to obtain Se films on commercial copper sheets (9–14 cm<sup>2</sup> exposed area) the electrodeposition was carried out in a two-electrode cell for 1-2 h under potentiostatic control at 60°C. The Pt plate with large surface area was the counterelectrode. Before electrolysis the substrate surface was cleaned appropriately and after plating the samples were rinsed with water and dried. A scanning electron microscope Quanta Inspect F (FEI-Philips) equipped with energy dispersion X-rays spectroscopy (EDX, Mn K $\alpha$  resolution at 132 eV), was used to determine surface morphology and elemental composition of Se deposits.

## 3. Results and discussion

Regarding the solubility process of selenium dioxide precursor in ChCl-urea, ChCl-EG or ChCl-OxA ionic liquids we suppose that Se<sup>4+</sup> free ions occur in the electrolyte, according to the following scheme:



However, the presence of chloride anion  $\text{Cl}^-$  as ligand forming complexes in ionic liquid can lead to conversion of  $\text{SeCl}_4$  into an anionic species of  $[\text{SeCl}_{4+x}]^{x-}$  type:



The most probable stoichiometry of this chlorocomplex has  $x=2$ , therefore  $\text{SeCl}_6^{2-}$  anions may be formed; the process is similar to complexing process in other ionic liquids for obtaining  $\text{TeCl}_6^{2-}$  species [46].

### 3.1. Cyclic voltammetry of selenium ions in ionic liquids containing choline chloride

CV technique has the advantage that charge transfer processes for Se electrodeposition can be recorded and characterized in terms of electrode potential and current density of cathodic peaks. Thus, before electrochemical preparation of Se films we proposed to study the reduction of  $\text{Se}^{4+}$  using this technique at constant temperature ( $60^\circ\text{C}$ ) in ChCl-urea, ChCl-EG and ChCl-OxA ionic liquids. In previous CV studies using these three media as solvents [47,48] we showed that any supplementary electrode process except the cathodic reduction of cholinium ion and anodic oxidation of  $\text{Cl}^-$ , which both are components of background electrolyte, does not appeared. However, it is worth mentioning that the electrochemical window in the eutectic mixture of choline chloride with oxalic acid (ChCl-OxA) used here is in general narrowed due to the presence of water molecules provided from dihydrated oxalic acid [47].

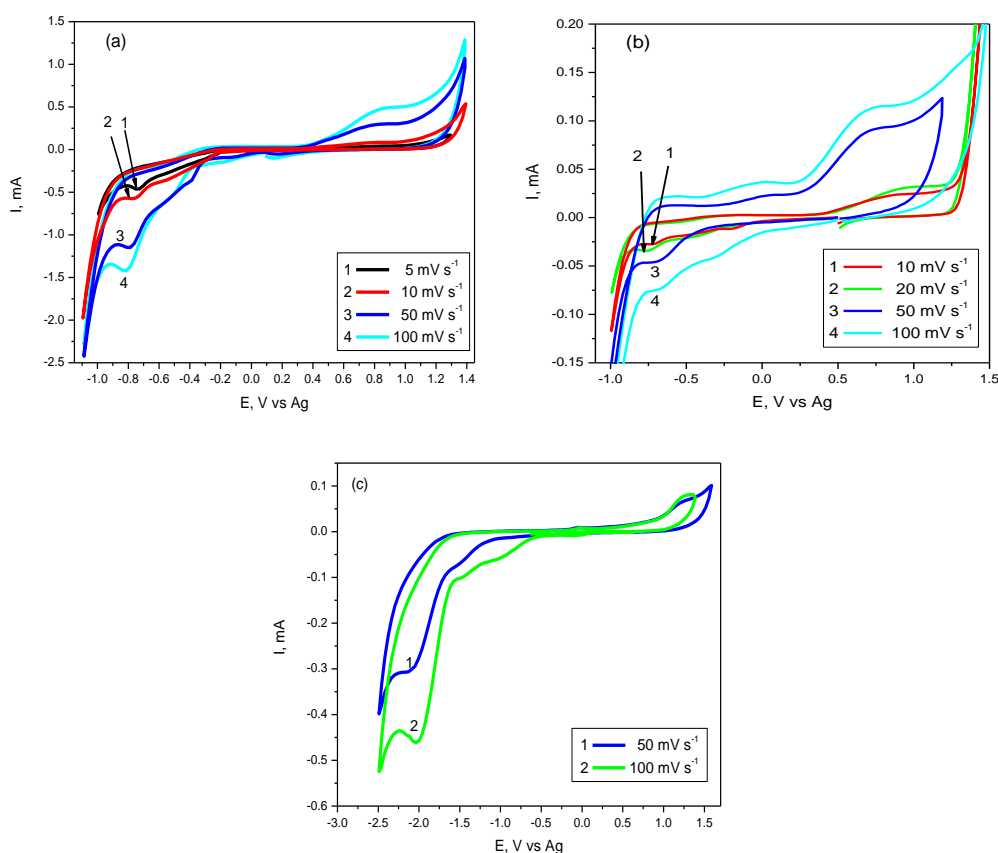


Fig. 1. Selected CVs from ChCl-urea + 10 mM  $\text{SeO}_2$  on different electrodes:  
 (a) Pt plate, scan rates: (1) 5; (2) 10; (3) 50 and (4) 100  $\text{mV s}^{-1}$ ;  
 (b) Pt disk, scan rates: (1) 10; (2) 20; (3) 50 and (4) 100  $\text{mV s}^{-1}$ ;  
 (c) GC disk, scan rates: (1) 50 and (2) 100  $\text{mV s}^{-1}$ .

A selection of the typical CV curves obtained on platinum and glassy carbon from ChCl-urea + SeO<sub>2</sub> systems is displayed in Figures 1. The scan of potential is first performed in negative direction. The shape of cathodic branch of voltammograms indicates a multiple reduction process with currents that increase with scan rate. Either a single or several reduction peaks or waves were recorded during the first scanned portion and they are attributed to underpotential deposition of selenium (Se-UPD). Further, the prominent cathodic peaks recorded on Pt plate or Pt disk in Figs. 1 a and 1 b are located in a potential range from -0.55 to -0.75 V and correspond to massive (bulk) deposition of selenium.

Similar to electrolysis in aqueous media or traditional ionic liquids we consider that the electroreduction of selenium ions takes place as a four-electron transfer, which is the process (1) above described. We may also consider in the case of SeCl<sub>6</sub><sup>2-</sup> anion reduction a four-electron transfer:



The massive process of Se deposition was hardly observed on GC electrode (Fig. 1 c), being rather a wave (from -1 to -1.5 V) in a more negative potential range than in voltammograms on Pt. Moreover, onto the inert GC surface a further reduction of Se<sup>0</sup> deposit into soluble species (Se<sup>2-</sup>) is evidenced by the peaks in Fig. 1 c between -2 and -2.2 V as a final reduction process (2) also discussed above.

As the anodic response in CV curves shows, the deposition of Se film tends to partially passivate surface for both Pt and GC electrodes. By returning the scan, the main oxidation peaks situated at 0.8 V or 0.9 V represent the stripping dissolution of selenium deposit. This very large peak potential difference, with  $\Delta E_p$  values from 1.6 up to 3 V, is a proof for an irreversible Se<sup>4+</sup>/Se<sup>0</sup> couple from electrochemically point of view, in spite of a probable diffusion control.

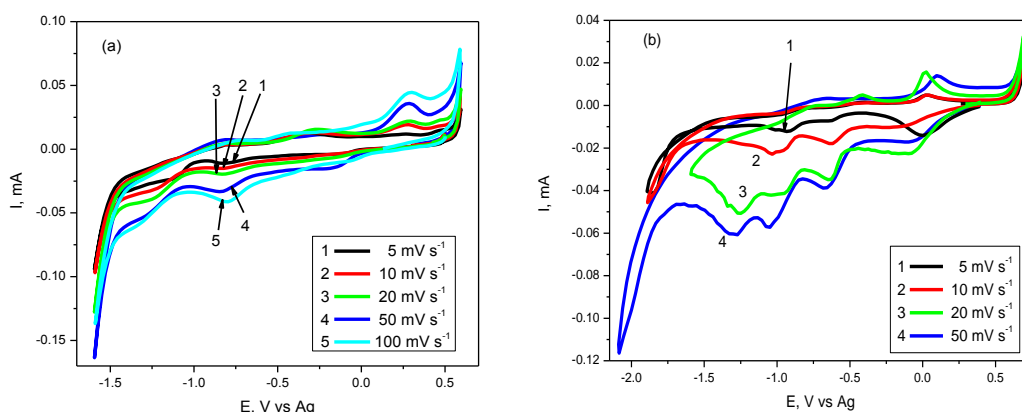


Fig. 2. CVs from ChCl-EG + 10 mM SeO<sub>2</sub> on different electrodes:  
 (a) Pt disk, scan rates: (1) 5; (2) 10; (3) 20; (4) 50 and (5) 100 mVs<sup>-1</sup>;  
 (b) GC disk, scan rates: (1) 5; (2) 10; (3) 20 and (4) 50 mVs<sup>-1</sup>.

CVs curves obtained from ChCl-EG + SeO<sub>2</sub> electrolytes are shown in Figs. 2 and 3. Based on previous discussion regarding the processes in ChCl-urea, the assignment of the cathodic peaks or waves recorded in Fig. 2 may be similar: underpotential deposition of selenium element (plateaus or peaks up to -0.7 V on Pt and up to -0.8 V on GC), its bulk deposition (peaks at around -0.8 V on Pt and around -1.1 V on GC), and formation of Se<sup>2-</sup>-soluble species (waves from -1.2 to -1.4 V on Pt and peaks between -1.25 and -1.35 V on GC). The last process (3) may lead to a supplementary precipitation of Se, process (4) [30]. The observed anodic peaks during the reverse scan in Fig. 2 may correspond to the successive oxidation of Se precipitate, Se bulk deposited and Se-UPD, respectively.

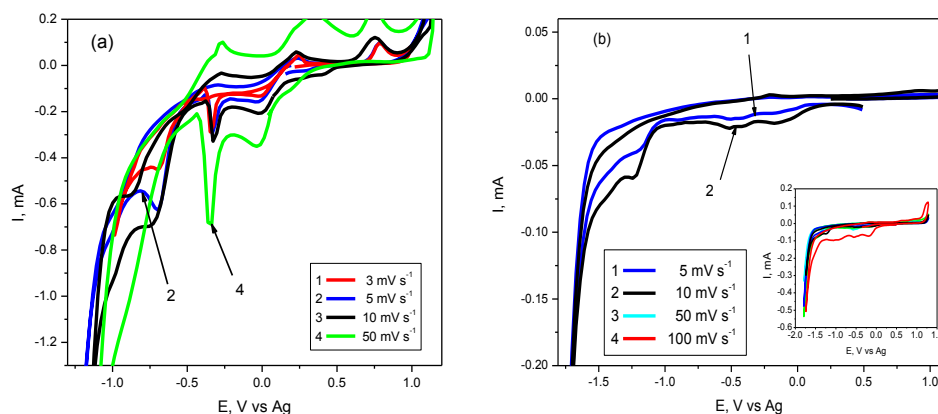


Fig. 3. Selected CVs from ChCl-EG + 15 mM SeO<sub>2</sub>: (a) on Pt plate, scan rates: (1) 5; (2) 10; (3) 20 and (4) 50 mVs<sup>-1</sup>; (b) on GC disk, scan rates: (1) 5; (2) 10; (3) 50 and (4) 100 mVs<sup>-1</sup>; in insertion: CV curves recorded on the total range of potentials

Figs. 3 present, similar to Figs. 2, the three cathodic processes recorded in the approximately same regions of potentials as for system with 10 mM Se<sup>4+</sup>. Higher current densities ( $i_p$ ) of all peaks or shoulders are due to higher SeO<sub>2</sub> concentration in electrolyte. Clearly, the currents for Se-UPD process remain constant with increasing scan rate, but the currents assigned to bulk Se<sup>0</sup> deposition, at potential around -0.7 V on Pt and -1.2 V on GC, have higher values with increasing scan rate ( $v$ ). The linear dependences of  $i_p$  with  $v^{1/2}$  and Se<sup>4+</sup> concentration (not shown here) suggest a diffusion controlled process for Se bulk deposition in ChCl-EG ionic liquids.

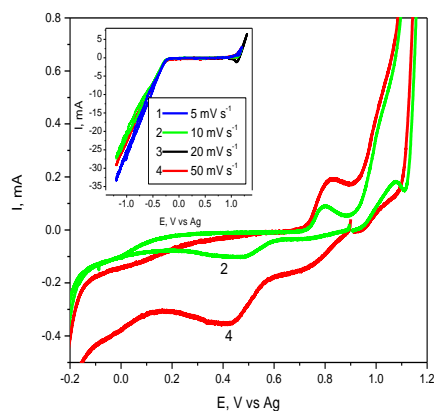


Fig. 4. Selected CVs on Pt plate from ChCl-OxA + 5 mM SeO<sub>2</sub> recorded in the potential range of Se-UPD and bulk deposition processes. In insertion: all CVs showing the limits of scanning

More complex are cathodic processes in the eutectic mixture of choline chloride with oxalic acid (ChCl-OxA) in which there were found smaller values (with 500 mV lower) of the electrochemical window than in ChCl-urea and ChCl-EG systems [47]. The window is certainly narrowed in the presence of around 13 wt% water introduced as hydrated oxalic acid. Thus, for ChCl-OxA + SeO<sub>2</sub> electrolytes an easier hydrogen evolution at the cathode is expected together with selenium deposition process. A selection of the voltammograms obtained on Pt electrode from 5 mM and 10 mM SeO<sub>2</sub> precursor dissolved in ChCl-OxA ionic liquid is showed in Figures 4 and 5. Successive cathodic peaks and waves are observed within the potential range from the start scanning (0.9 V) up to -0.2 V, and they are assigned to Se-UPD processes. The bulk (massive) deposition of selenium takes place only at potentials more negative than -0.3 V, illustrated in general as a continuous increasing of cathodic current. For instance, the shoulder located around

-0.35 V in Fig. 5 may be attributed to this deposition process (process 1). On the anodic branch of voltammograms in Figs. 4 and 5 a single peak at cca 0.84 V is the main oxidation process that is attributed to electrochemical dissolution of selenium deposit.

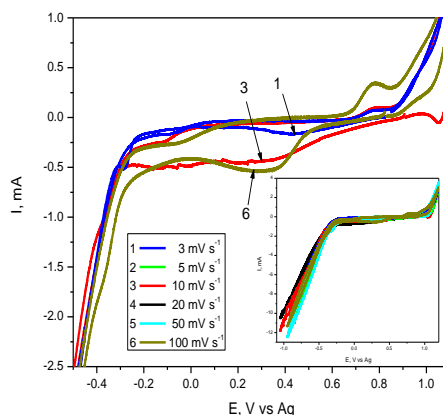
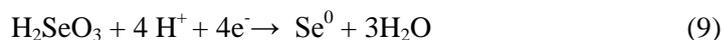


Fig. 5. Selected CVs on Pt plate from ChCl-OxA + 10 mM SeO<sub>2</sub> recorded in the potential range of Se-UPD and bulk deposition processes. In insertion: all CVs showing the limits of scanning

However, taking into account the significant presence of water another pathway of the process of selenium deposition is possible by considering the selenous acid H<sub>2</sub>SeO<sub>3</sub> as participant species to reduction, even partially. As it was presented in the literature of aqueous solutions [27,30,49] the selenium can be also deposited from the process:



Obviously, it is expected for both processes (1) and (9) to have lower current yields because they are accompanied with an intensive hydrogen evolution.

### 3.2. Microscopy and EDX analysis of selenium deposited films

Based on the above CV studies on platinum and glassy carbon electrodes, selenium thin films were electrodeposited on copper sheets in conditions of controlled potential at constant temperature of 60°C. We conducted a series of experiments in unstirred solutions containing ChCl-urea, ChCl-EG and ChCl-OxA as solvents and SeO<sub>2</sub> dissolved precursor, in order to correlate the film composition and morphology with the electrodeposition parameters. Crystalline and adherent deposits of dark grey colour were obtained by applying a potential step starting from the stationary potential (E<sub>stat</sub>) of each electrode/electrolyte interface.

Table 1 presents the electrolysis conditions (nature of bath, stationary electrode potential, applied electrode potential, time duration and temperature) and results of EDX elemental analysis for as-prepared Se samples. The content of oxygen and chlorine elements as impurities is likely originated from ionic liquid incorporated during electrodeposition or which was not fully removed from the final surface of film. This explains the fact that selenium film deposited from ChCl-urea electrolyte (which has the largest viscosity among investigated ionic liquids) had the highest content of impurities. In addition, a part of the oxygen impurity may come from the oxidation in air of freshly deposited selenium before the sample to be analysed by SEM/EDX.

A comparison of SEM pictures at high magnification (Figs. 6) shows very different morphology which depends primarily on the nature of electrolytic bath and less on the amplitude of cathodic step (polarization value). Thus, in Fig. 6 a small grains of selenium grown from ChCl-urea ionic liquid seem to come together into big aggregates like a coalescence effect. The film is the thinnest and non-uniform distributed onto the substrate surface.

Table 1. EDX results regarding impurities of Se films prepared with potential control from various ionic liquids based on choline chloride

Elements	Content found by EDX analysis	
	wt%	at%
Electrolyte: <b>ChCl-urea + 10 mM SeO<sub>2</sub></b> Electrolysis at -0.235 V ( $E_{\text{stat}} = -0.170$ V vs. Ag ref.) for 1 h, 60°C		
Se K	21.59	5.71
O K	67.18	87.69
Cl K	11.23	6.60
Electrolyte: <b>ChCl-EG + 15 mM SeO<sub>2</sub></b> Electrolysis at -0.350 V ( $E_{\text{stat}} = -0.238$ V vs. Ag ref.) for 1 h, 60°C		
Se K	79.56	44.08
O K	20.44	55.92
Electrolyte: <b>ChCl-EG + 15 mM SeO<sub>2</sub></b> Electrolysis at -0.450 V ( $E_{\text{stat}} = -0.238$ V vs. Ag ref.) for 1 h, 60°C		
Se K	72.72	35.06
O K	27.28	64.94
Electrolyte: <b>ChCl-OxA + 5 mM SeO<sub>2</sub></b> Electrolysis at -0.320 V ( $E_{\text{stat}} = -0.277$ V vs. Ag ref.) for 2 h, 60°C		
Se K	44.12	13.79
O K	55.88	86.21
Electrolyte: <b>ChCl-OxA + 10 mM SeO<sub>2</sub></b> Electrolysis at -0.320 V ( $E_{\text{stat}} = -0.262$ V vs. Ag ref.) for 1.5 h, 60°C		
Se K	87.86	59.45
O K	12.14	40.55

In Figs. 6 b,c the morphologies of films deposited from ChCl-EG at two polarization potentials are similar, although a more dense film is obtained by increasing the cathodic polarization from -0.350 to -0.450 V. The deposits show worm-like elongated microcrystals (vermicular shape) that are uncurled and have in general more than 100 nm length. On contrary, the uniform deposits formed in ChCl-OxA ionic liquid (Figs. 6 d,e) show cubic or quite polygonal microcrystals with dimensions around 15-40 nm. As it can be seen the grains are somehow agglomerated, but with a higher degree of unification for the bath with 10 mM SeO<sub>2</sub>.

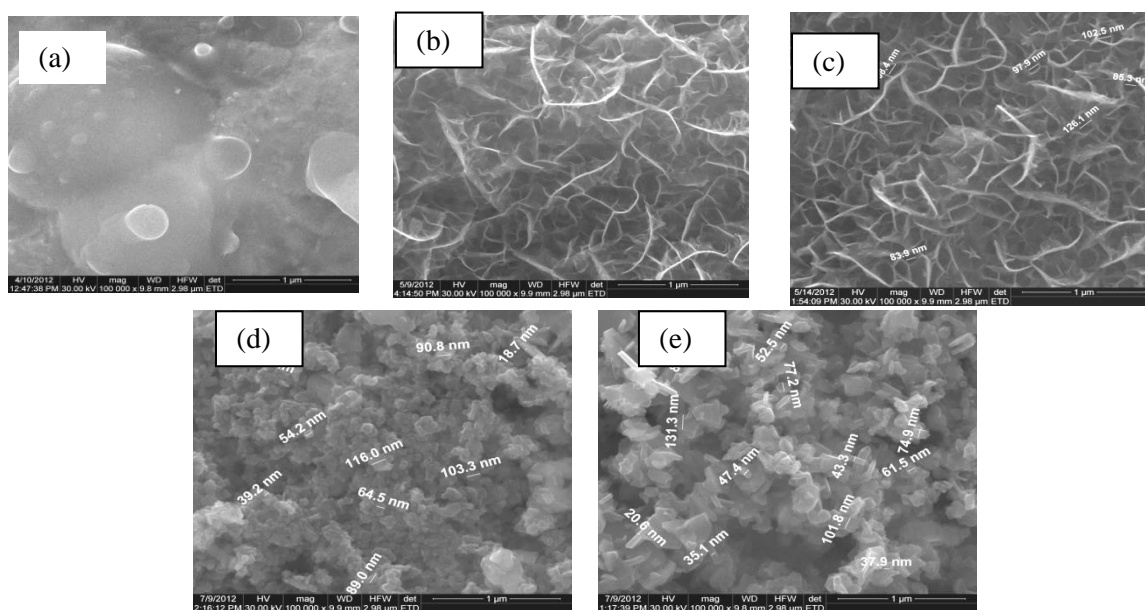


Fig. 6. Comparative SEM images of Se films electrodeposited on Cu at 60°C from various ionic liquids: (a) ChCl-urea + 10 mM SeO<sub>2</sub>; (b) ChCl-EG + 15 mM SeO<sub>2</sub>, polarization at -0.350 V; (c) ChCl-EG + 15 mM SeO<sub>2</sub>, polarization at -0.450 V; (d) ChCl-OxA + 5 mM SeO<sub>2</sub>; (e) ChCl-OxA + 10 mM SeO<sub>2</sub>. The preparation details were indicated in Table 1.

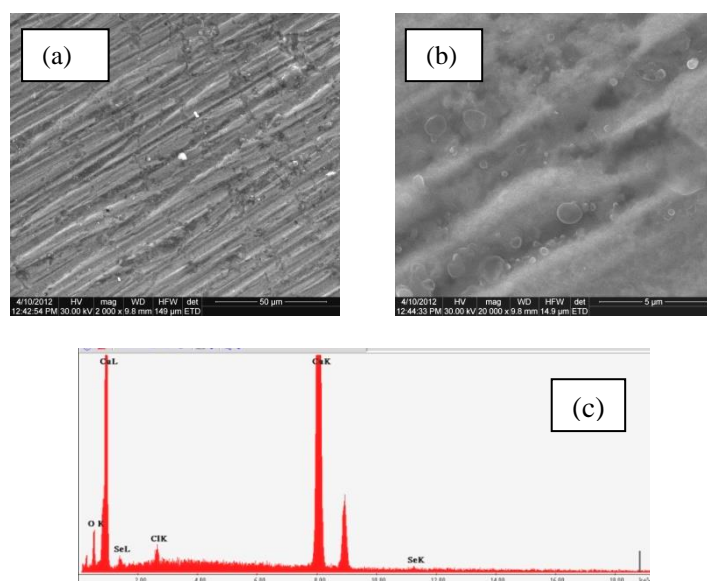


Fig. 7. SEM images (a,b) of selenium film electrodeposited on Cu from ChCl-urea + 10 mM SeO<sub>2</sub>; (c) EDX pattern. See Table 1 for preparation conditions

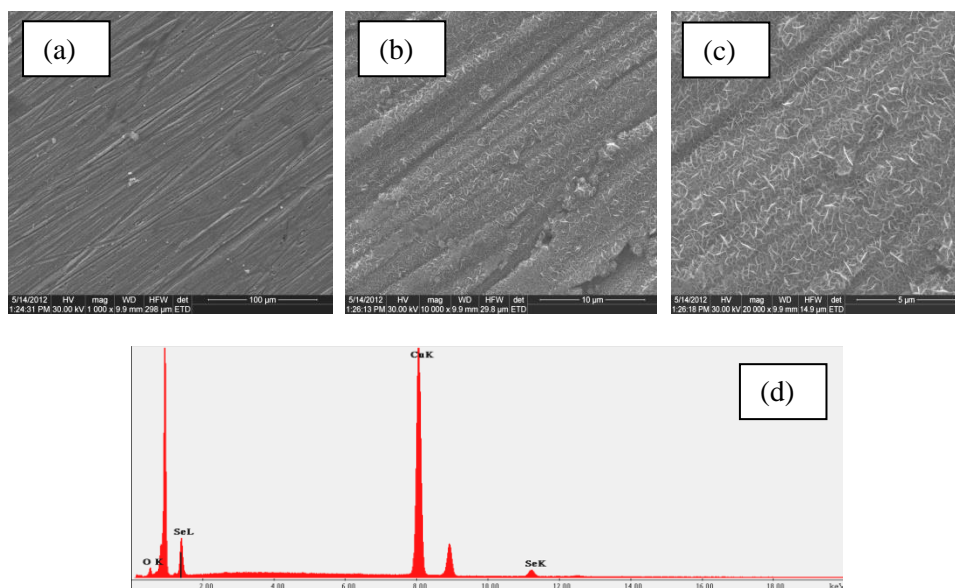


Fig. 8. SEM images (a-c) of selenium film electrodeposited on Cu from ChCl-EG + 15 mM SeO<sub>2</sub> at -0.450 V applied potential; (d) EDX spectrum. See Table 1 for preparation conditions

SEM pictures at different magnifications and EDX patterns for as-deposited Se films are shown in details in Figures 7-10. Figs. 7 a,b show that Se film grown from ChCl-urea covers completely the substrate surface, although it is very thin. An analysis of EDX pattern for film deposited from this bath reveals a high penetration of the incident X-ray beam that led to significant amplitude of peaks for Cu substrate (Fig. 7 c). A chlorine peak is also observed together with a higher peak assigned to oxygen.

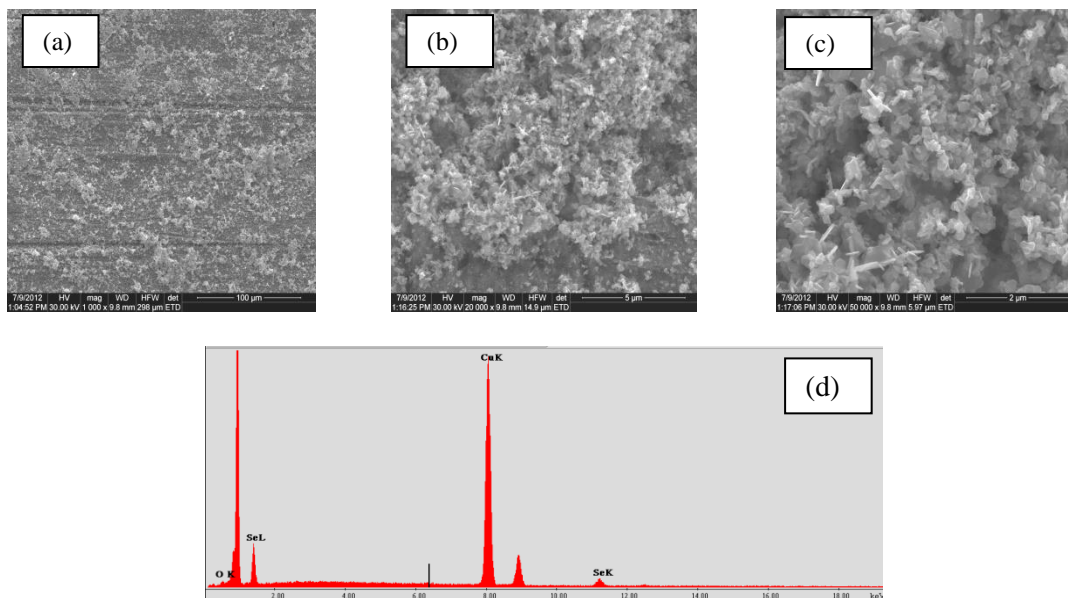


Fig. 9. (a-c) SEM images of selenium film electrodeposited on Cu from ChCl-OxA + 5 mM SeO<sub>2</sub>; (d) EDX spectrum. See Table 1 for preparation conditions

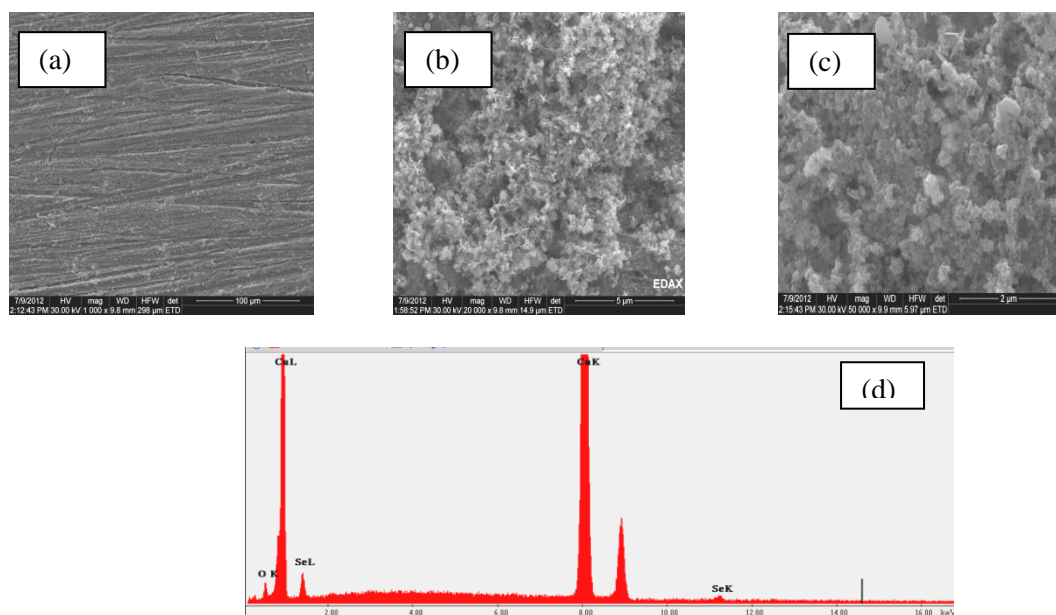


Fig. 10. (a-c) SEM images of selenium film electrodeposited on Cu from ChCl-OxA + 10 mM SeO<sub>2</sub>; (d) EDX spectrum. See Table 1 for preparation conditions

Figs. 8-10 show that more compact and coherent Se films were grown from ChCl-EG + 15 mM SeO<sub>2</sub> and ChCl-OxA + 10 mM SeO<sub>2</sub> electrolytes. Accordingly, the EDX peaks ascribed to the substrate material (Cu) and oxygen content were attenuated in the patterns. As Table 1 shows, the most rich in selenium were the samples prepared from ChCl-OxA + 10 mM SeO<sub>2</sub> (cca 88 wt% Se) at -0.320 V and from ChCl-EG + 15 mM SeO<sub>2</sub> at -0.350 V (cca 80 wt% Se), respectively.

#### 4. Conclusions

Se deposits could be obtained electrochemically from the three investigated ionic liquids based on eutectic binary mixtures of choline chloride (ChCl) with the hydrogen donor compounds as urea, ethylene glycol (EG) or oxalic acid (OxA), respectively. Cyclic voltammograms on platinum and glassy carbon showed that successive processes of underpotential deposition, bulk deposition and conversion of  $\text{Se}^0$  into a soluble species ( $\text{Se}^{2-}$ ) take place by gradual scanning of cathodic potential to more negative values. SEM images indicated morphology with coalescent spherical aggregates of Se microcrystals for Se film grown in ChCl-urea + 10 mM  $\text{SeO}_2$ , which had the lowest thickness. More compact and coherent Se films were grown from ChCl-EG + 15 mM  $\text{SeO}_2$  and ChCl-OxA + 10 mM  $\text{SeO}_2$  but their morphologies are different, with vermicular or cubic (polygonal) grains, respectively. The richest films in selenium were obtained if they are deposited with controlled potentials at -0.320 V in ChCl-OxA+ 10 mM  $\text{SeO}_2$  (cca 88 wt% Se) and -0.350 V in ChCl-EG + 15 mM  $\text{SeO}_2$  (cca 80 wt% Se), respectively.

#### References

- [1] R.K. Pandey, S.N. Sahu, S. Chandra, Handbook of Semiconductor Electrodeposition, Marcel Dekker, New York, 1996.
- [2] M. Bouroushian, Electrochemistry of Metal Chalcogenides, Springer, Berlin, 2010, 57.
- [3] S.-Y. Zhang, J. Zhang, Y. Liu, X. Ma, H.-Y. Chen, Electrochim. Acta **50**, 4365 (2005).
- [4] X.Y. Zhang, Y. Cai, J.Y. Miao, K.Y. Ng, Y.F. Chan, X.X. Zhang, N. Wang, J. Cryst. Growth **276**(3-4), 674 (2005).
- [5] M.F. Cabral, H.B. Suffredini, V.A. Pedrosa, S.T. Tanimoto, S.A.S. Machado, Appl. Surf. Sci. **254**(17), 5612 (2008).
- [6] S. Kumar, J. Exp. Nanosci. **4** (4), 341(2009).
- [7] A.R. Ingole, S. R. Thakare, N.T. Khati, A.V. Wankhade, D.K. Burghate, Chalcog. Lett., **7** (7), 485 (2010).
- [8] M.N. Sokolov, Metal chalcogenides: clusters, layers, nanotubes (chapter 9.1), in: F. Devillanova, W.W. Du Mont (Eds), Handbook of Chalcogen Chemistry: New Perspectives in Sulfur, Selenium and Tellurium, Vol. 1, 2<sup>nd</sup> edition, RSC Publ., Cambridge, 2013, 475.
- [9] B. He, W. Zhang, II-VI Semiconductors and their device applications (chapter 11.4), in: F. Devillanova, W.W. Du Mont (Eds), Handbook of Chalcogen Chemistry: New Perspectives in Sulfur, Selenium and Tellurium, Vol. 2, 2<sup>nd</sup> edition, RSC Publ., Cambridge, 2013, 180.
- [10] I. Nandhakumar, J.M. Elliott, G.S. Attard, Electrodeposition of nanostructured mesoporous selenium films, in: M.P. Soriaga, J. Stickney, L.A. Bottomley, Y.G. Kim (Eds), Thin Films: Preparation, Characterization, Applications, Kluwer Academic/Plenum Publ., New York, 2002, 113.
- [11] M.W. George, chapter 65: Selenium and Tellurium, in: U.S. Geological Survey Minerals Yearbook 2003.
- [12] L. Ren, H. Zhang, P. Tan, Y. Chen, Z. Zhang, Y. Chang, J. Xu, F. Yang, D. You, J. Phys. Chem. B **108**, 4627 (2004).
- [13] V.S. Minaev, S.P. Timoshenkov, V.V. Kalugin, J. Optoelectron. Adv. Mater. **7**(4), 1717 (2005).
- [14] M.A. Malik, K. Ramasamy, P. O'Brien, Selenium and tellurium containing precursors for semiconducting materials (chapter 9), in: J.D. Woollins, R. Laitinen (Eds), Selenium and Tellurium Chemistry: From Small Molecules to Biomolecules and Materials, Springer, Berlin, 2011, 201.
- [15] H. Chen, Y.M. Yeh, S.T. Huang, W.J. Yeh, Chalcog. Lett. **10** (7), 229 (2013).
- [16] Y.M. Yeh, H. Chen, S.H. Wang, S.T. Huang, Y.J. Chen, Chalcog. Lett. **11** (1), 29 (2014).
- [17] C. Wei, N. Myung, K. Rajeshwar, J. Electroanal. Chem. **375**, 109 (1994).
- [18] T.E. Lister, J.L. Stickney, J. Phys. Chem. **100** (50), 19568 (1996).
- [19] B.M. Huang, T.E. Lister, J.L. Stickney, Surf. Sci. **392**, 27 (1997).
- [20] S. Cattarin, M. Musiani, J. Electroanal. Chem. **437** (1-2), 85 (1997).

- [21] P. Zuman, G. Somer, *Talanta* **51** (4), 645 (2000).
- [22] M. Bouroushian, T. Kosanovic, Z. Loizos, N. Spyrellis, *Electrochem. Commun.* **2** (4), 281 (2000).
- [23] G. Pezzatini, F. Loglio, M. Innocenti, M.L. Foresti, *Collect. Czech. Chem. Commun.* **68** (9), 1579 (2003).
- [24] M. Alanyalioglu, U. Demir, C. Shannon, *J. Electroanal. Chem.* **561**, 21 (2004).
- [25] M.C. Santos, S.A.S. Machado, *J. Electroanal. Chem.* **567** (2), 203 (2004).
- [26] M.O. Solaliendres, A. Manzoli, G.R. Salazar-Banda, K.I.B. Eguiluz, S.T. Tanimoto, S.A.S. Machado, *J. Solid State Electrochem.* **12** (6), 679 (2008).
- [27] M.F. Cabral, V.A. Pedrosa, S.A.S. Machado, *Electrochim. Acta* **55** (3), 1184 (2010).
- [28] Y. Lai, F. Liu, J. Li, Z. Zhang, Y. Liu, *J. Electroanal. Chem.* **639** (1-2), 187 (2010).
- [29] A. Steponavicius, D. Simkunaite, I. Valsiunas, G. Baltrunas, *Chemija* **22**, 91 (2011).
- [30] R. Kowalik, *Arch. Metall. Mater.* **59** (3), 871 (2014).
- [31] S. Zein El Abedin, A.Y. Saad, H.K. Farag, N. Borisenko, Q.X. Liu, F. Endres, *Electrochim. Acta* **52**, 2746 (2007).
- [32] N. Borisenko, S. Zein El Abedin, F. Endres, chapter 6, *Electrodeposition of semiconductors in ionic liquids*, in: *Electrodeposition of Metals from Ionic Liquids*, F. Endres, A.P. Abbott, D. MacFarlane (Eds.), Wiley-VCH, Weinheim, 2008, 161.
- [33] S. Zein El Abedin, F. Endres, chapter 7 in: *Molten Salts and Ionic Liquids. Never the Twain?*, M. Gaune-Escard, K.R. Seddon (Eds.), J. Wiley & Sons, New York, 2010, 85.
- [34] A. Abdel Aal, R. Al-Salman, M. Al-Zoubi, N. Borisenko, F. Endres, O. Höfft, A. Prowald, S. Zein El Abedin, *Electrochim. Acta* **56** (28), 10295 (2011).
- [35] A. Abdel Aal, F. Voigts, D. Chakarov, F. Endres, *Electrochim. Acta* **59**, 228 (2012).
- [36] A. Abdel Aal, F. Voigts, D. Chakarov, F. Endres, *J. Solid State Electrochem.* **16**, 3027 (2012).
- [37] L.H. Chou, I.W. Sun, C.L. Hussey, *ECS Trans.* **33**, 575 (2010).
- [38] M. Steichen, P. Dale, *Electrochem. Commun.* **13**, 865 (2011).
- [39] A.P. Abbott, D.L. Davies, G. Capper, R.K. Rasheed, V. Tambyrajah, *Ionic liquids and their use as solvents*, US Patent 2004/0097755 A1, May 20, 2004.
- [40] D.D. Shivagan, P.J. Dale, A.P. Samantilleke, L.M. Peter, *Thin Solid Films* **515** (15), 5899 (2007).
- [41] M. Bougouma, A. Van Elewyck, M. Steichen, C. Buess-Herman, T. Doneux, *J. Solid State Electrochem.* **17**, 527 (2013).
- [42] A. Cojocaru, M. Sima, *Rev. Chim. (Bucharest)* **63**, 217 (2012).
- [43] C. Agapescu, A. Cojocaru, F. Golgovici, A.C. Manea, A. Cotarta, *Rev. Chim. (Bucharest)* **63** (9), 911 (2012).
- [44] C. Agapescu, A. Cojocaru, A. Cotarta, T. Visan, *Chalcog. Lett.* **9** (10), 403 (2012).
- [45] F. Golgovici, T. Visan, M. Buda, *Chalcog. Lett.* **10** (6), 197 (2013).
- [46] R.W. Tsai, Y.T. Hsieh, P.Y. Chen, I.W. Sun, *Electrochim. Acta* **137**, 49 (2014).
- [47] C. Agapescu, A. Cojocaru, A. Cotarta, T. Visan, *J. Appl. Electrochem.* **43** (3), 309 (2013).
- [48] M.L. Mares Badea, A. Cojocaru, L. Anicai, *UPB Sci. Bull. Series B* **76** (3), 21 (2014).
- [49] R. Kowalik, K. Fitzner, *J. Electroanal. Chem.* **633**, 78 (2009).